



THE UNIVERSITY *of* EDINBURGH

## Edinburgh Research Explorer

### Multi-decadal observations of the Antarctic Ice Sheet from restored analog radar records

**Citation for published version:**

Schroeder, DM, Dowdeswell, JA, Siegert, M, Bingham, RG, Chu, W, Mackie, EJ, Siegfried, MR, Vega, KI, Emmons, JR & Winstein, K 2019, 'Multi-decadal observations of the Antarctic Ice Sheet from restored analog radar records', *Proceedings of the National Academy of Sciences (PNAS)*.  
<https://doi.org/10.1073/pnas.1821646116>

**Digital Object Identifier (DOI):**

[10.1073/pnas.1821646116](https://doi.org/10.1073/pnas.1821646116)

**Link:**

[Link to publication record in Edinburgh Research Explorer](#)

**Document Version:**

Publisher's PDF, also known as Version of record

**Published In:**

Proceedings of the National Academy of Sciences (PNAS)

**General rights**

Copyright for the publications made accessible via the Edinburgh Research Explorer is retained by the author(s) and / or other copyright owners and it is a condition of accessing these publications that users recognise and abide by the legal requirements associated with these rights.

**Take down policy**

The University of Edinburgh has made every reasonable effort to ensure that Edinburgh Research Explorer content complies with UK legislation. If you believe that the public display of this file breaches copyright please contact [openaccess@ed.ac.uk](mailto:openaccess@ed.ac.uk) providing details, and we will remove access to the work immediately and investigate your claim.



# Multidecadal observations of the Antarctic ice sheet from restored analog radar records

Dustin M. Schroeder<sup>a,b,1</sup>, Julian A. Dowdeswell<sup>c</sup>, Martin J. Siegert<sup>d</sup>, Robert G. Bingham<sup>e</sup>, Winnie Chu<sup>a</sup>, Emma J. MacKie<sup>a</sup>, Matthew R. Siegfried<sup>a,2</sup>, Katherine I. Vega<sup>a</sup>, John R. Emmons<sup>f</sup>, and Keith Winstein<sup>b,f</sup>

<sup>a</sup>Department of Geophysics, Stanford University, Stanford, CA 94305; <sup>b</sup>Department of Electrical Engineering, Stanford University, Stanford, CA 94305; <sup>c</sup>Scott Polar Research Institute, University of Cambridge, CB2 1ER Cambridge, United Kingdom; <sup>d</sup>Grantham Institute, Imperial College London, SW7 2AZ London, United Kingdom; <sup>e</sup>School of GeoSciences, University of Edinburgh, EH8 9XP Edinburgh, United Kingdom; and <sup>f</sup>Department of Computer Science, Stanford University, Stanford, CA 94305

Edited by Eric Rignot, University of California, Irvine, CA, and approved August 8, 2019 (received for review December 19, 2018)

**Airborne radar sounding can measure conditions within and beneath polar ice sheets. In Antarctica, most digital radar-sounding data have been collected in the last 2 decades, limiting our ability to understand processes that govern longer-term ice-sheet behavior. Here, we demonstrate how analog radar data collected over 40 y ago in Antarctica can be combined with modern records to quantify multidecadal changes. Specifically, we digitize over 400,000 line kilometers of exploratory Antarctic radar data originally recorded on 35-mm optical film between 1971 and 1979. We leverage the increased geometric and radiometric resolution of our digitization process to show how these data can be used to identify and investigate hydrologic, geologic, and topographic features beneath and within the ice sheet. To highlight their scientific potential, we compare the digitized data with contemporary radar measurements to reveal that the remnant eastern ice shelf of Thwaites Glacier in West Antarctica had thinned between 10 and 33% between 1978 and 2009. We also release the collection of scanned radargrams in their entirety in a persistent public archive along with updated geolocation data for a subset of the data that reduces the mean positioning error from 5 to 2.5 km. Together, these data represent a unique and renewed extensive, multidecadal historical baseline, critical for observing and modeling ice-sheet change on societally relevant timescales.**

Antarctica | radio echo sounding | glaciology | remote sensing | archival data

The greatest source of uncertainty in estimates of future sea-level rise is the contribution of continental ice sheets (1). A fundamental obstacle to providing robust sea-level projections on the decadal-to-century timescales used in assessment and planning is our poor understanding of subsurface and ice-shelf processes in the potentially unstable marine sectors of Antarctica where retreating ice would encounter deepening water (2). However, unlike surface-elevation and ice-velocity data, which can be derived from satellites to produce long-spanning, continent-scale, and repeat time series (3, 4), direct observations of ice thickness and subsurface conditions at the glacier-catchment to ice-sheet scales are only possible from airborne ice-penetrating radar-sounding surveys (5). Unfortunately, the cost and logistics involved in these surveys have resulted in much of the Antarctic subsurface being observed on only a single occasion (6). An extensive, early ice-penetrating radar survey, collected in the 1970s by an international collaboration between the Scott Polar Research Institute (SPRI) at the University of Cambridge, the National Science Foundation (NSF), and the Technical University of Denmark (TUD) was recorded on optical film reels, which were physically stored at the SPRI in Cambridge (7, 8) (Fig. 1). These data provide a benchmark against which more recent data can be compared to assess changes in ice thickness and subsurface conditions. However, even in regions where repeat observations do exist (9–11), most of the airborne sounding data have been collected in the last 2 decades and have yet to be used for longer

timescale analysis due to the limited availability and fidelity of the archival film data. In this paper, we address this challenge by scanning and releasing the entire film record along with updated posting for a subset of the data. We illustrate the range of ice-sheet subsurface features captured in these records and demonstrate how they can be used to investigate temporal change even in regions with relatively poor initial or updated geolocation.

The SPRI/NSF/TUD radar-sounding survey, collected from 1971 to 1979, produced over 400,000 line-km of subsurface profiles (7, 8, 12, 13). The radar system operated at center frequencies of 60 MHz and/or 300 MHz with aircraft positioning calculated using an inertial navigation system with a reported accuracy of 5 km (8) registered to an internal Coded Binary Decimal (CBD) clock/counter. Radar traces were processed onboard using an analog implementation of pulse compression and unfocused synthetic aperture radar processing. The resulting fast-time gradient in returned power was log-detected and recorded on 35-mm optical film as “Z-scope” radargram profiles. These original analog radar profiles and their interpretation at the time were instrumental

## Significance

One of the greatest challenges in projecting the sea-level contributions of ice sheets over the next century is the lack of observations of conditions within and underneath the ice sheet that span more than a decade or two. By digitizing archival ice-penetrating radar data recorded in the 1970s on 35-mm optical film, we can compare modern and archival radar-sounding data at their full resolution in order to observe changes in the Antarctic ice sheet over more than 40 y. This makes it possible to investigate and model subsurface processes over both large scales and several decades for the first time.

Author contributions: D.M.S. designed research; D.M.S. performed research; D.M.S., W.C., E.J.M., M.R.S., K.I.V., J.R.E., and K.W. analyzed data; and D.M.S., J.A.D., M.J.S., R.G.B., W.C., E.J.M., M.R.S., K.I.V., and K.W. wrote the paper.

The authors declare no conflict of interest.

This article is a PNAS Direct Submission.

This open access article is distributed under [Creative Commons Attribution-NonCommercial-NoDerivatives License 4.0 \(CC BY-NC-ND\)](#).

Data deposition: All of the radargrams reported in the paper as well as the entire collection of the scanned radargrams are available on the persistent public Stanford Digital Repository (SDR) at [doi.org/10.25740/ykq4-9345](https://doi.org/10.25740/ykq4-9345). This includes the original Scott Polar Research Institute (SPRI) flight-based metadata for latitude, longitude, ice thickness, and surface elevation—registered to Coded Binary Decimal (CBD) counter—where available with a reported 5-km positioning accuracy. This archive also includes our flight-based updated cross-correlation-based positioning—also registered to CBD—with estimated <2.5-km positioning accuracy. A more user-friendly interface to the scans and positioning data are also available at <https://exhibits.stanford.edu/radarfilm>.

<sup>1</sup>To whom correspondence may be addressed. Email: [dustin.m.schroeder@stanford.edu](mailto:dustin.m.schroeder@stanford.edu).

<sup>2</sup>Present address: Department of Geophysics, Colorado School of Mines, Golden, CO 80401.

This article contains supporting information online at [www.pnas.org/lookup/suppl/doi:10.1073/pnas.1821646116/-DCSupplemental](http://www.pnas.org/lookup/suppl/doi:10.1073/pnas.1821646116/-DCSupplemental).

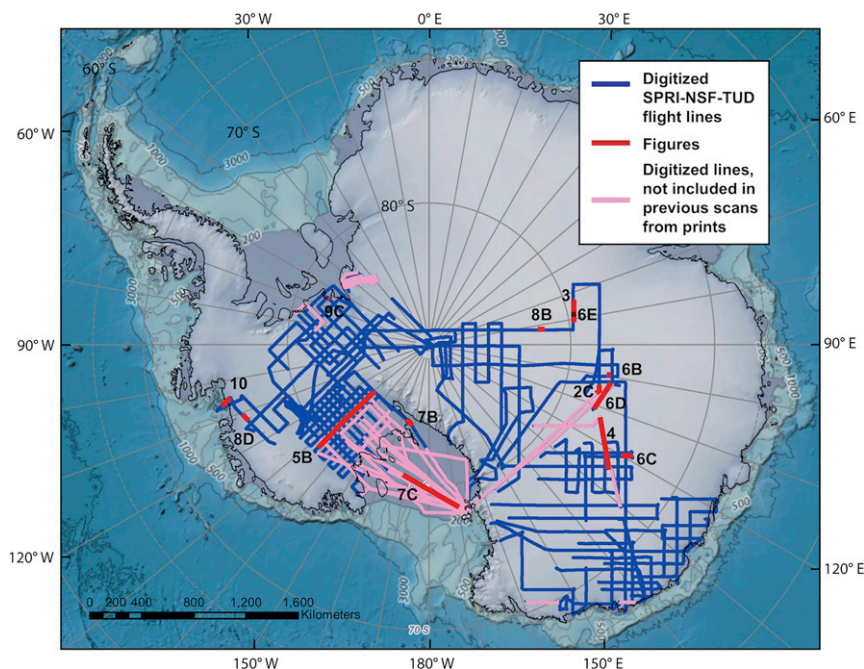


**Fig. 1.** Film scanning coverage improvement. Scanned radar-sounding film records span both the East and West Antarctic ice sheets. Flight lines of the high-resolution scanned radar film, including 25% never scanned previously at any resolution (pink lines) (12).

in the discovery and early understanding of, for example, subglacial lakes (14, 15), ice-shelf processes (16, 17), ice-core climate records (18), and the topography of the underlying continent (6, 19). Since then, modern digital descendants of this system have also been used to investigate regional volcanism (20), englacial structures including ice-sheet stratigraphy and freeze-on features (21), and subsurface melting (9). However, the complete, digitized, high resolution data set has not been released to a persistent public archive, despite its foundational role in Antarctic glaciology and a previous effort that scanned photographic prints from a subset of the survey (12, 22).

Our goals are to describe and demonstrate the utility of the SPRI/NSF/TUD radar records in multidecadal analyses and to produce high-resolution scans of the entire 35-mm-film archive fully available to enable systematic continent-scale syntheses of high-quality archival and modern radar-sounding data. This dataset improves the coverage, resolution, and geolocation of radar profiles available for inclusion in interpolated bed-topography maps of Antarctica and for the interpretation of subglacial and englacial features in the radargrams. A principal challenge for any quantitative or multitemporal analysis using this dataset is the accuracy of its geolocation, which had an estimated mean error of <5 km from inertial navigation when collected (8) and which hampers temporal change detection if uncorrected. We have reduced that error to an average of 2.5 km through cross-correlation with contemporary sounding data for a subset of the survey (6) (*Methods*). This will continue to improve as additional data are collected and the radargrams and thickness profiles that make up gridded datasets (e.g., ref. 6) are released. However, even with the existing geolocation, finer-scale registration and interpretation are possible at or near the inherent range (meters) and azimuth resolution of the radargrams (10s of meters) if distinct features can be identified. We demonstrate this type of long-baseline, profile-based, geolocation-insensitive comparison with contemporary glaciological observations by investigation of ocean-driven processes beneath 2 West Antarctic ice shelves.

The improved coverage (Fig. 1), georectification, spatial resolution, and radiometric sensitivity (Fig. 2) of the scanned film record highlights the greater fine-scale (<1 km) topographic information (Fig. 3) available from our scans of the same SPRI/NSF/TUD data

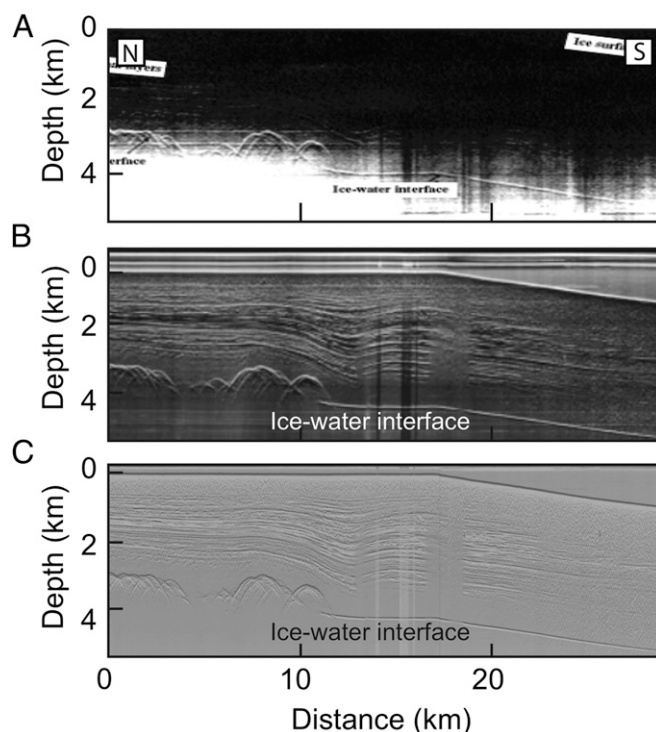


**Fig. 2.** Film scanning resolution improvement. (A) Published radar film print of the Lake Vostok region originally acquired in 1974 (15). (B) Intermediate resolution scan of radar film print of the same portion of film (12). (C) High-resolution direct scan of the same portion of film in greater resolution—this report.



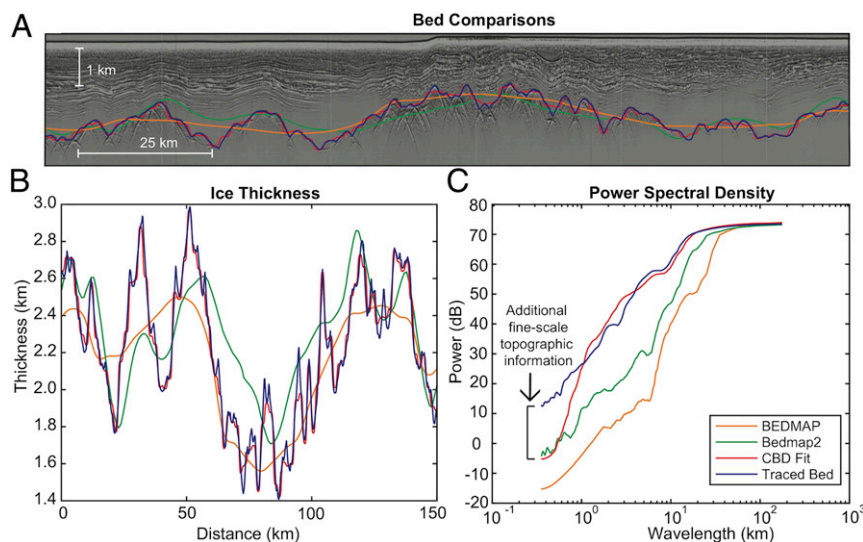


**Fig. 3.** Example of improved-resolution bed topography from digitized historic radar film. (A) A 60-MHz 1978 Z-scope radar profile in the Gamburtsev Mountains with topography from BEDMAP (19) (orange), Bedmap2 (6) (green), interpolation of thickness measurements at the spacing of A-scope traces (cubic interpolation based on CBD clock/counter 2.5 km spacing) (19) (red) and tracing the bed in the Z-scope radargram (blue). (B) The resulting ice-thickness profiles. (C) The power spectra of these basal profiles.

(blue line in Fig. 3) when compared with those included in existing bed-topography datasets (6, 19); this includes both the smoothed topography in the gridded products (orange and green lines in Fig. 3) and in the presmoothed A-scope or “CBD-spaced” (*Methods*) profiles used in those products (red line in Fig. 3). This topographic information will enable both retrospective and prognostic ice-sheet modeling aimed at improved understanding of basal motion, grounding-line stability, and other processes that are sensitive to basal roughness and fine-scale topography (23).

The improved geometric and radiometric resolution of the scans also enhances the interpretability of a wide range of englacial and basal ice-sheet features. This includes profiles with englacial layers that connect ice core age–depth relationships (e.g., ref. 18) with the enhanced range resolution (Fig. 4). Additionally, the improved resolution and coverage of the scans also enable the construction of contiguous cross-sections of the Siple Coast ice streams (Fig. 5), among others, and the expansion

of subglacial lake inventories (e.g., ref. 22) to include smaller lakes that have previously been difficult to resolve (Fig. 6). Much of the film record that has been scanned (Fig. 1) was recorded over ice shelves and their grounding zones, particularly the Ross Ice Shelf (Fig. 7). Ice shelves can evolve dramatically over decadal timescales (e.g., ref. 9) and can now be investigated by comparison with contemporary surveys (24). The scans also reveal unique features that have been identified in modern radar-sounding data but were previously unidentified in the SPRI film record, such as accretion bodies (21) and englacial ash layers (20) (Fig. 8), or ice-shelf basal channels (25) (Fig. 9).

Beyond enhancing radargram interpretation and fine-scale topographic information, the digitized film records provide a powerful historical baseline to compare with modern radar-sounding data. These records enable measurements of changes in ice thickness, englacial features, and basal conditions over time spans approaching or exceeding 40 y. For example, our scans include a profile from 1978 data (Fig. 9) over an ice-shelf

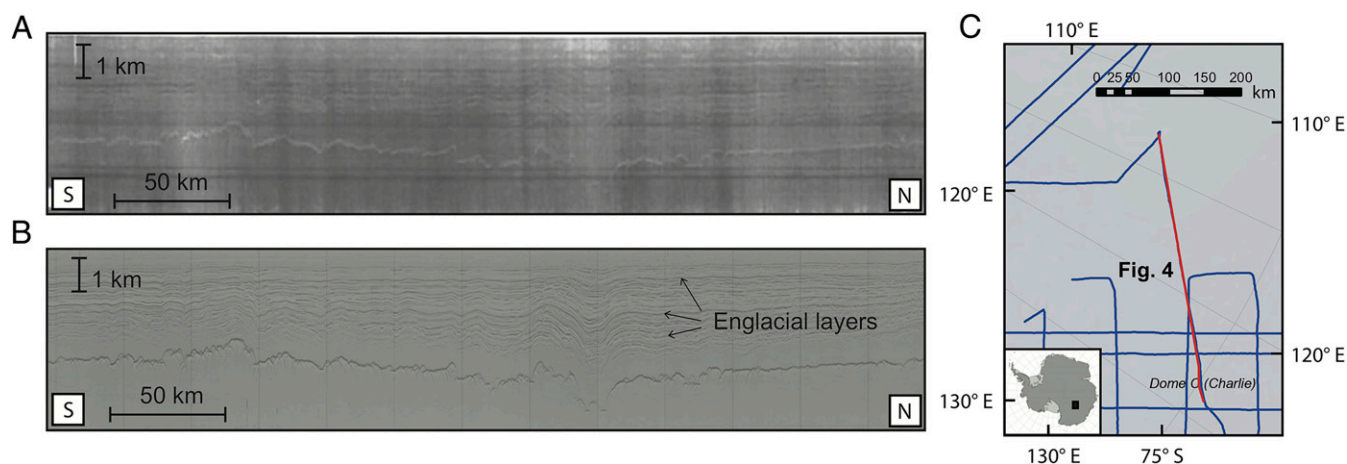


**Fig. 4.** Enhanced englacial layer record. (A) A 1974 60-MHz profile of englacial radar layers used to connect the englacial stratigraphy to ice core age records from the Dome C and Vostok Ice Cores (18). (B) The same profile scanned with the greater geometric and radiometric resolution provided by our study, revealing deeper and more continuous layers. (C) Map of profile location.











accuracies could be attainable using radargram misfits that exploit both bed and englacial layer geometries as more profile-based sounding data are collected or released. This release of archival radar scans includes both the original and updated positioning.

The absolute positioning of the film record can be further enhanced in the multitemporal comparison of specific ice-sheet features in one or more radar-sounding profile by identifying and analyzing distinctly interpretable features in the profiles. In these cases, the recorded SPRI navigation (or improved positioning) can be treated as an initial coarse location envelope within which specific features in the archival radargrams can be identified and analyzed at the inherent resolution of the profile (meters in range and 10s of meters in azimuth).

We demonstrate this approach with a FRIS basal channel (Fig. 9), which is a distinct feature, and can therefore be located precisely in the along-profile direction. As a result, the remaining cross-profile (along-channel) positioning error of 8 km ( $\pm 4$  km) would lead to a channel height estimate error of  $<2\%$  if the apparent contemporary local along-flow height gradient of  $\sim 0.5\text{ km}^{-1}$  inferred from surface altimetry was stable over the 40 y period of observation (25).

Similarly, for the TEIS (Fig. 10), we can overcome the fact that the 2009 radar-sounding profiles are not direct refights of the 1979 SPRI line by analyzing the distribution of ice thicknesses in the portion of the shelf that is

interpreted to be floating (identified by basal crevassing and regrounding signatures in the sounding profiles and therefore insensitive to positioning uncertainty) rather than directly differencing profiles. We also use 2 profiles from 2009 (one of which crosses the SPRI survey near the grounding line and the other which crosses it near the regrounding point) to bound the lateral variability in ice-shelf thickness. This lateral variability results in an estimated uncertainty of 2–20 m between lines on a thinning signal of 115 m. In the future, direct refights of the SPRI lines (e.g., ref. 9) could result in much richer, less ambiguous observations of subsurface change.

The L1B OIB MCoRDS radargrams were obtained from the CREStIS, University of Kansas (26, 27) available for download from <https://data.cresis.ku.edu/data/rds/>.

**ACKNOWLEDGMENTS.** The authors would like to thank the staff of the SPRI, University of Cambridge, especially Naomi Boneham, Lucy Martin, and Toby Benham as well as Jessica Daniel and Matthew Chalker for their assistance in accessing, scanning, and rearchiving the radar films. We also thank David Drewry for helping uncover the meaning of the CBD acronym. D.M.S. and E.J.M. were supported, in part, by an NSF CAREER Award. W.C. was supported, in part, by a grant from the NASA Cryospheric Sciences Program. M.R.S. was supported by the George Thompson Fellowship at Stanford University, a grant from the NASA Cryospheric Sciences Program.

1. T. F. Stocker *et al.*, Eds., *IPCC, 2013: Climate Change 2013: The Physical Science Basis. Contribution of Working Group I to the Fifth Assessment Report of the Intergovernmental Panel on Climate Change* (Cambridge University Press, Cambridge, United Kingdom and New York, NY, USA, 2013).
2. T. A. Scambos *et al.*, How much, how fast?: A science review and outlook for research on the instability of Antarctica's Thwaites Glacier in the 21st century. *Global Planet. Change* **153**, 16–34 (2017).
3. F. S. Paolo, H. A. Fricker, L. Padman, Ice sheets. Volume loss from Antarctic ice shelves is accelerating. *Science* **348**, 327–331 (2015).
4. E. Rignot *et al.*, Four decades of Antarctic ice sheet mass balance from 1979–2017. *Proc. Natl. Acad. Sci. U.S.A.* **116**, 1095–1103 (2019).
5. J. A. Dowdeswell, S. Evans, Investigations of the form and flow of ice sheets and glaciers using radio-echo sounding. *Rep. Prog. Phys.* **67**, 1821–1861 (2004).
6. P. Fretwell *et al.*, Bedmap2: Improved ice bed, surface and thickness datasets for Antarctica. *Cryosphere* **6**, 4305–4361 (2013).
7. G. de Q. Robin, D. J. Drewry, D. T. Meldrum, International studies of ice sheet and bedrock. *Philos. Trans. R. Soc. Lond. B Biol. Sci.* **279**, 185–196 (1977).
8. D. J. Drewry, S. R. Jordan, E. Jankowski, Measured properties of the Antarctic ice sheet: Surface configuration, ice thickness, volume and bedrock characteristics. *Ann. Glaciol.* **3**, 83–91 (1982).
9. A. Khazendar *et al.*, Rapid submarine ice melting in the grounding zones of ice shelves in West Antarctica. *Nat. Commun.* **7**, 13243 (2016).
10. W. Chu *et al.*, Extensive winter subglacial water storage beneath the Greenland ice sheet. *Geophys. Res. Lett.* **43**, 12,484–12,492 (2016).
11. D. M. Schroeder, A. M. Hilger, J. D. Paden, D. A. Young, H. F. J. Corr, Ocean access beneath the southwest tributary of Pine Island Glacier, West Antarctica. *Ann. Glaciol.* **59**, 10–15 (2017).
12. R. G. Bingham, M. J. Siegert, Radio-echo sounding over polar ice masses. *J. Environ. Eng. Geophys.* **12**, 47–62 (2007).
13. D. J. Drewry, *Antarctica: Glaciological and Geophysical Folio* (Scott Polar Research Institute, University of Cambridge, 1983).
14. G. K. A. Oswald, G. d. Q. Robin, Lakes beneath the Antarctic ice sheet. *Nature* **245**, 251–254 (1973).
15. M. J. Siegert, J. K. Ridley, An analysis of the ice-sheet surface and subsurface topography above the Vostok Station subglacial lake, central East Antarctica. *J. Geophys. Res.* **103**, 10195–10207 (1998).
16. C. S. Neil, Radio echo determination of basal roughness characteristics on the Ross Ice Shelf. *Ann. Glaciol.* **3**, 216–221 (1982).
17. R. D. Crabtree, C. S. M. Doake, Radio-Echo investigations of Ronne Ice Shelf. *Ann. Glaciol.* **8**, 37–41 (1986).
18. M. J. Siegert, R. Hodgkins, J. A. Dowdeswell, A chronology for the Dome C deep ice-core site through radio-echo layer correlation with the Vostok Ice Core, Antarctica. *Geophys. Res. Lett.* **25**, 1019–1022 (1998).
19. M. B. Lythe, D. G. Vaughan, BEDMAP: A new ice thickness and subglacial topographic model of Antarctica. *J. Geophys. Res. Solid Earth* **106**, 11335–11351 (2001).
20. A. C. Lough *et al.*, Seismic detection of an active subglacial magmatic complex in Marie Byrd Land, Antarctica. *Nat. Geosci.* **6**, 1031–1035 (2013).
21. R. E. Bell *et al.*, Widespread persistent thickening of the East Antarctic ice sheet by freezing from the base. *Science* **331**, 1592–1595 (2011).
22. M. J. Siegert, J. A. Dowdeswell, M. Gorman, N. F. McIntyre, An inventory of Antarctic subglacial lakes. *Antarct. Sci.* **8**, 281–286 (1996).
23. G. Durand, O. Gagliardini, L. Favier, T. Zwinger, E. le Meur, Impact of bedrock description on modeling ice sheet dynamics. *Geophys. Res. Lett.* **38**, L20501 (2011).
24. K. J. Tinto *et al.*, Ross Ice Shelf response to climate driven by the tectonic imprint on seafloor bathymetry. *Nat. Geosci.* **12**, 441–449 (2019).
25. A. M. Le Brocq *et al.*, Evidence from ice shelves for channelized meltwater flow beneath the Antarctic ice sheet. *Nat. Geosci.* **6**, 945–948 (2013).
26. C. Leuschen, updated 2018. IceBridge MCoRDS L1B Geolocated Radar Echo Strength Profiles (Version 2, NASA National Snow and Ice Data Center Distributed Active Archive Center, Boulder, Colorado, 2014). <https://nsidc.org/data/IRMC1B/versions/2>. Accessed 5 January 2018.
27. C. Leuschen, J. Paden, P. Gogineni, F. Rodriguez-Morales, C. Allen, IceBridge MCoRDS L1B geolocated radar echo strength profiles, version 1 (NASA National Snow and Ice Data Center, Boulder, CO, 2011), IRMC1B.
28. K. J. Tinto, R. E. Bell, Progressive unpinning of Thwaites Glacier from newly identified offshore ridge: Constraints from aerogravity. *Geophys. Res. Lett.* **38**, L20503 (2011).
29. J. Mouginot, E. Rignot, B. Scheuchl, Sustained increase in ice discharge from the Amundsen Sea Embayment, West Antarctica, from 1973 to 2013. *Geophys. Res. Lett.* **41**, 1576–1584 (2014).
30. J. A. MacGregor, G. A. Catania, M. S. Markowski, A. G. Andrews, Widespread rifting and retreat of ice-shelf margins in the eastern Amundsen Sea Embayment between 1972 and 2011. *J. Glaciol.* **58**, 458–466 (2011).
31. M. P. Schodlok, D. Menemenlis, E. Rignot, M. Studinger, Sensitivity of the ice-shelf/ocean system to the sub-ice-shelf cavity shape measured by NASA IceBridge in Pine Island Glacier, West Antarctica. *Ann. Glaciol.* **53**, 156–162 (2012).
32. E. Rignot, S. Jacobs, J. Mouginot, B. Scheuchl, Ice-shelf melting around Antarctica. *Science* **341**, 266–270 (2013).
33. M. A. Depoorter *et al.*, Calving fluxes and basal melt rates of Antarctic ice shelves. *Nature* **502**, 89–92 (2013).
34. A. Jenkins *et al.*, West Antarctic ice sheet retreat in the Amundsen Sea driven by decadal oceanic variability. *Nat. Geosci.* **11**, 733–738 (2018).
35. D. M. Schroeder *et al.*, Data from “Stanford-Cambridge radar film digitization project.” Stanford Digital Repository. <https://doi.org/10.25740/ykq4-9345>. Deposited 31 October 2018.
36. J. T. Bailey, S. Evans, G. de Q. Robin, Radio echo sounding of polar ice sheets. *Nature* **204**, 420–421 (1964).
37. S. Evans, G. d. Q. Robin, Glacier depth-sounding from the air. *Nature* **210**, 883–885 (1966).
38. P. Gudmandsen, Layer echoes in polar ice sheets. *J. Glaciol.* **15**, 95–101 (1975).
39. J. A. Dowdeswell, M. J. Siegert, The dimensions and topographic setting of Antarctic subglacial lakes and implications for large-scale water storage beneath continental ice sheets. *Geol. Soc. Am. Bull.* **111**, 254–263 (1999).
40. J. A. Dowdeswell, M. J. Siegert, The physiography of modern Antarctic subglacial lakes. *Global Planet. Change* **35**, 221–236 (2003).
41. J. S. Greenbaum *et al.*, Ocean access to a cavity beneath Totten Glacier in East Antarctica. *Nat. Geosci.* **8**, 294–298 (2015).
42. T. Wrona *et al.*, Position and variability of complex structures in the central East Antarctic ice sheet. *Geol. Soc. Spec. Publ.* **461**, 113–129 (2018).
43. K. E. Alley, T. A. Scambos, M. R. Siegfried, H. A. Fricker, Impacts of warm water on Antarctic ice shelf stability through basal channel formation. *Nat. Geosci.* **9**, 290–293 (2016).